

## S1 Validation of the depth-averaging tool

The depth-averaging tool is validated on a simple geometrical configuration, consisting of a rigid block sliding on an inclined plane and then falling from a cliff. The plane is inclined at an angle  $\theta_{\text{plane}} = 30^\circ$  and has an inclined length of  $L_{\text{plane}} = 22$  m from the tail of the block. The cliff has height  $H_{\text{cliff}} = 10$  m above a horizontal plane.

The block has height  $H_{\text{block}} = 0.1$  m and length  $L_{\text{block}} = 0.3$  m. The MPM simulation is initialized with the block vertically shifted by two grid sizes,  $2 \cdot gs = 0.02$  m, to avoid the block sticking to the plane. Simulations are performed on a topography with cell size of  $cs = 0.01$  m and results are exported with a resolution  $cs_e = cs$ .

Figure S1a shows the computed flow height  $h$  and thickness  $t$  (both projected normal to the topography) at  $t_e = 0$ , determined using Eqs. 7 and 8, respectively. The computed thickness  $t$  varies between 0 and 0.1 m, being constantly equal to 0.1 m where the top face of the block vertically projects within the basal face of the block. Similarly, the computed depth  $h$  varies between 0 and 0.12 m, this latter value being due to the vertical translation by  $2 \cdot gs$  above the topography. Some oscillations are here observed, which may be due to the irregular sampling of material points. On the entire right-side of the block, the flow depth remains equal to  $\approx 0.1$  m, which is because the algorithm performs the particles search in a vertical direction, and the block is here overhanging (see discussion in Sec. 2.3.2). In summary, the computed initial flow heights are well calculated by the code.

As the block moves down along the inclined plane, and then falls from the cliff, the theoretical flow thickness can be calculated as:

$$\begin{cases} t = H_{\text{block}}, & \text{if } x < L_{\text{plane}} \cos \theta_{\text{plane}} \\ H_{\text{block}} \leq t \leq \sqrt{L_{\text{block}}^2 + H_{\text{block}}^2}, & \text{if } x \geq L_{\text{plane}} \cos \theta_{\text{plane}} \end{cases} \quad (\text{S1})$$

where the last condition is because the block rotates during the free fall and might therefore be thicker than  $H_{\text{block}}$ . The blue line in Figure S1b (maximum value of  $t$  over all time steps) shows good agreement with Eq. S1; note the slight increase of  $t_{\text{max}}$  towards the end of the free fall, which is also when we observe the block rotating in the MPM simulation.

The theoretical flow depth can be calculated as:

$$\begin{cases} h \approx H_{\text{block}}, & \text{if } x < L_{\text{plane}} \cos \theta_{\text{plane}} \\ h \approx H_{\text{block}} + H_{\text{cliff}} - \tan \theta_{\text{plane}}(x - L_{\text{plane}} \cos \theta_{\text{plane}}) - \frac{1}{2}g \frac{(x - L_{\text{plane}} \cos \theta_{\text{plane}})^2}{v_{\text{term}}^2 \cos^2 \theta_{\text{plane}}}, & \text{if } x \geq L_{\text{plane}} \cos \theta_{\text{plane}} \end{cases} \quad (\text{S2})$$

where  $g$  is the acceleration due to gravity and  $v_{\text{term}}$  is the final speed of the block on the plane:

$$v_{\text{term}} = \sqrt{2gL_{\text{plane}} \sin \theta_{\text{plane}}}. \quad (\text{S3})$$

The red line in Figure S1b (maximum value of  $h$  over all time steps) shows good agreement with Eq. S2.

The theoretical slope-parallel speed can be calculated as:

$$\begin{cases} u_t = \sqrt{2gx \tan \theta_{\text{plane}}}, & \text{if } x < L_{\text{plane}} \cos \theta_{\text{plane}} \\ u_t \approx v_{\text{term}} \cos \theta_{\text{plane}}, & \text{if } x \geq L_{\text{plane}} \cos \theta_{\text{plane}} \end{cases} \quad (\text{S4})$$

The cyan line in Figure S1c (maximum value of  $u_t$  (Eq. 14) over all time steps) shows reasonable agreement with Eq. S4. However, the computed slope-parallel velocity slightly underestimates the theoretical one. We checked the MPM results by examining the particles' velocities at the end of the inclined plane, and the observed discrepancy can be attributed to numerical dissipations inherent in the APIC numerical scheme. Instead, the depth-averaging tool seems to export the correct results for the slope-parallel speed. Note that in the two cells located immediately before and after the cliff, the calculated value of  $u_t$  dips. This reduction is linked to the abrupt terrain transition, which influences the computation of the spatial gradients of the surface, as defined in Eq. 4a. As a result, the surface normals (Eq. 3) in these two cells are nearly horizontal. Consequently, while the normal slope velocity increases above 0 in these two cells (not visible in Figure S1d because it is out of scale), the slope-parallel velocity correspondingly experiences a decrease.

The theoretical slope-normal speed can be calculated as:

$$\begin{cases} u_n = 0, & \text{if } x < L_{\text{plane}} \cos \theta_{\text{plane}} \\ u_n \approx -v_{\text{term}} \sin \theta_{\text{plane}} - \frac{g(x - L_{\text{plane}} \cos \theta_{\text{plane}})}{v_{\text{term}} \cos \theta_{\text{plane}}}, & \text{if } x \geq L_{\text{plane}} \cos \theta_{\text{plane}} \end{cases} \quad (\text{S5})$$

The magenta line in Figure S1d (minimum value of  $u_n$  (Eq. 13) over all time steps) shows good agreement with Eq. S5. Some discrepancy is observed in the free fall from the cliff, which is again due to dissipations in the MPM scheme.

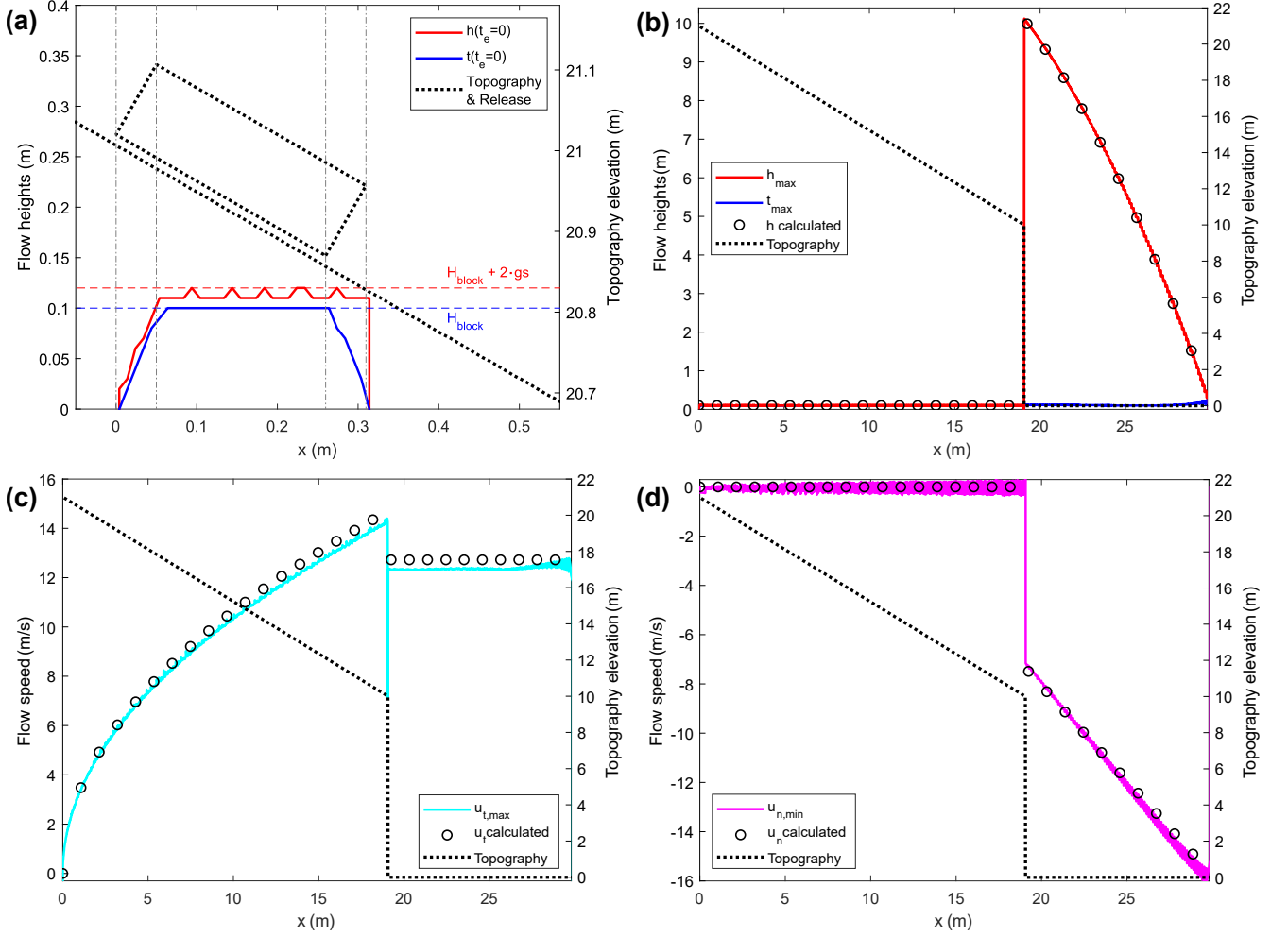


**Figure S1.** Validation of the depth-averaging code for a block sliding on an inclined plane and falling from a cliff. The computed flow variables are shown with coloured lines, while the calculated analytical solutions are shown with black circles. (a) Initial configuration and computed flow depth and thickness at  $t = 0$ . (b) Maximum flow depth and thickness over all time steps. (c) Maximum slope-parallel speed over all time steps. (d) Minimum slope-normal speed over all time steps.

## S2 Material parameters for the ice avalanche simulation

Table S1 shows all the parameters for the ice avalanche simulations.

**Table S1.** Parameters for ice avalanche MPM simulation of the Whymper serac fall in 1998.

Parameter	Value
Initial bulk and particles' density, $\rho_0$	850 kg/m <sup>3</sup>
Bulk modulus, $K$	6.7 MPa
Shear modulus, $G$	4.0 MPa
Initial friction angle, $\varphi_i$	40°
Residual friction angle, $\varphi_r$	20°
Initial cohesion, $c_i$	1 kPa
Basal friction, $\mu$	0.65 (glacier) – 0.55 (bedrock)
Softening coefficient, $\xi$	10
Grid size, $gs$	1 m
Points per cell, $n_g$	6

## S3 Flow detachment from the terrain

The depth-averaging algorithm enables us to capture flow detachment from the terrain, as observed in the slope-normal velocity component (Fig. 2h) and the difference between flow depth (measured from the terrain surface to the upper flow surface) and flow thickness (distance between the lowest and highest particles in a cell) (Fig. 2i). Figure 2i was computed using all particles (i.e., percentile set to P=100), including potentially scattered or isolated particles at the top of the flow.

To investigate the influence of filtering these outliers, we compare results obtained using different percentile values (P=20 to P=100), as shown in Fig. S2. Lower percentiles exclude the topmost particles, reducing both flow depth and flow thickness. In general, the trends along the profile remain similar regardless of the chosen percentile. In cells with sparse particle populations, percentile filtering has limited or no effect, as only a few particles are present (see Fig. S3). In zones where the flow is detached from the topography, using lower percentile values significantly reduces the flow thickness  $t$ , while the flow depth  $h$  remains comparatively stable, since it is still measured from the terrain to the upper percentile-bound particle. In contrast, in zones where the flow is attached to the terrain, changing the percentile value affects both flow depth and flow thickness in a similar way.

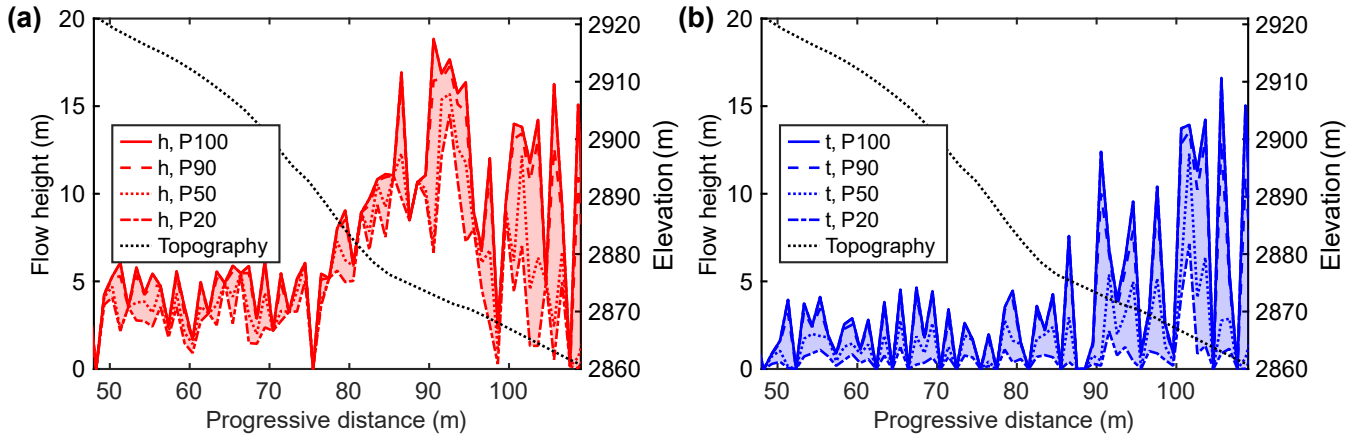


**Figure S2.** Flow depth (a) and flow thickness (b) exported with different percentile values. The shaded areas show the variability of the flow height metrics for the considered range (between P=20 and P=100).

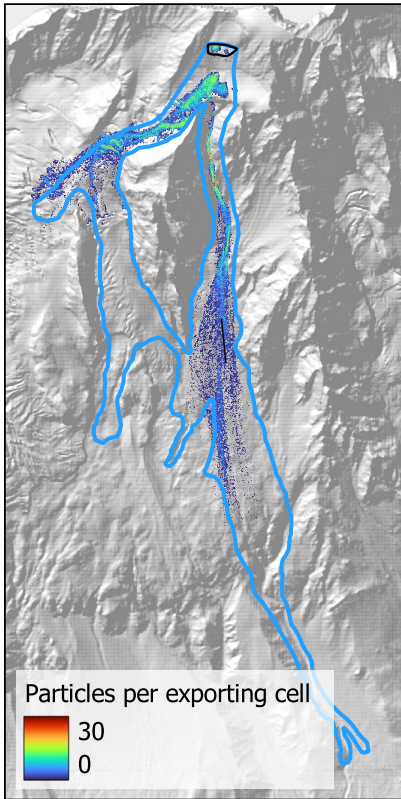


**Figure S3.** Number of particles per cell at  $t_e = 50$  s.